JACS
JOURNAL OF THE AMERICAN CHEMICAL SOCIETY
Article
pubs.acs.org/JACS

Hydrogen Bonded Arrays: The Power of Multiple Hydrogen Bonds

Alireza Shokri,[†] Jacob Schmidt,[†] Xue-Bin Wang,*[,‡] and Steven R. Kass*[,†]

[†]Department of Chemistry, University of Minnesota, Minneapolis, Minnesota 55455, United States

[‡]Chemical & Materials Sciences Division, Pacific Northwest National Laboratory, P.O. Box 999, MS K8-88 Richland, Washington 99352, United States, and Department of Physics, Washington State University, 2710 University Drive, Richland, Washington 99354, United States

Supporting Information

ABSTRACT: Hydrogen bond interactions in small covalent model compounds (i.e., deprotonated polyhydroxy alcohols) were measured by negative ion photoelectron spectroscopy. The experimentally determined vertical and adiabatic electron detachment energies for $(HOCH_2CH_2)_2CHO^-$ (**2a**), $(HOCH_2CH_2)_3CO^-$ (**3a**), and $(HOCH_2CH_2CH(OH)CH_2)_3CO^-$ (**4a**) reveal that hydrogen-bonded networks can provide enormous stabilizations and that a single charge center not only can be stabilized by up to three hydrogen bonds but also can increase the interaction energy between noncharged OH groups by 5.8 kcal mol^{-1} or more per hydrogen bond. This can lead to pK_a values that are very different from those in water and can provide some of the impetus for catalytic processes.

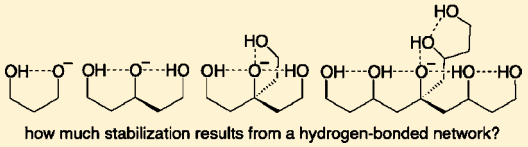

INTRODUCTION

Many enzymes catalyze a wide variety of chemical processes by using two or even three hydrogen bonds to a single oxygen atom in what is commonly referred to as an oxyanion hole (Figure 1).[1] The strength of the individual hydrogen bonds can vary considerably, and the presence of a strong low-barrier or single-well hydrogen bond has been used to explain a variety of enzyme mechanism pathways (e.g., mandelate racemase, triosephosphate isomerase, citrate synthase, and glycolate oxidase).[2] Additive effects involving two and three hydrogen bonds to one charged center also have been shown in several enzyme model systems.[3,4] However, networks of hydrogen bonds are employed by enzymes, and the energies of these additional interactions are important in catalysis but are not well understood.[5] In this report, negative-ion photoelectron spectroscopy is used to directly probe the energetic consequences of hydrogen bond arrays in small covalently bound model compounds and the experimental results are compared to computational predictions. We find that in a series of monodeprotonated polyhydroxy alcohols (i.e., polyols) the strengths of the hydrogen bond arrays systematically increase with the number of hydroxyl groups from 1 to 3 and for 6. That is, an oxygen anion center is stabilized most effectively by up to 3 hydrogen bond donors, but in the process the donor groups become better hydrogen bond acceptors. The resulting hydrogen-bonded network can provide a large energetic stabilization that may lead to catalytic rate enhancements and greater acidities and basicities than those measured in water.

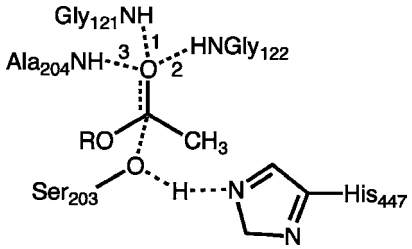

Figure 1. Proposed transition state for the enzymatic hydrolysis of acetylcholine with acetylcholinesterase via a three-pronged oxyanion hole (i.e., 1−3); see ref 1d for additional details.

EXPERIMENTAL SECTION

General. ^{1}H and ^{13}C NMR spectra were recorded on Varian VI-300, VXR-300, and VI-500 spectrometers and are reported in parts per million (δ). High-resolution mass spectral analyses were performed with a Bruker BioTof II electrospray ionization−time-of-flight mass spectrometer with an internal standard; a methanol solution of PEG polymer was used for this purpose. Medium pressure liquid chromatography (25−60 psi) was carried out on silica gel using a Biotage Isolera 1. Thin-layer chromatography (TLC) was performed on 0.25 mm Masherey-Nagel silica gel plates, and compounds were visualized using aqueous potassium permanganate or *p*-anisaldehyde (1% EtOH solution) stains.

2-Benzyl-1,3-diphenylpropan-2-ol. A dry three-necked round-bottomed flask was equipped with a magnetic stirring bar and an addition funnel, a reflux condenser with an argon inlet, and a rubber septum. The flask was charged with 6.90 g (0.283 mol) of magnesium turnings, and 200 mL of anhydrous diethyl ether. A solution of 17.56 g (0.156 mol) of benzyl chloride (Alfa Aesar) in 20 mL of diethyl ether was added dropwise over 45 min so as to maintain a gentle reflux. Subsequently, 4.50 g (0.050 mol) of dimethylcarbonate was added dropwise over a 20 min period and the resulting reaction mixture was stirred for an additional 20 h at room temperature before being quenched with 100 mL of 10% aqueous HCl. The resulting two layers were separated, and the aqueous solution was extracted three times with 100 mL of diethyl ether. The combined organic material was

Received: September 2, 2011
Published: December 22, 2011

   dx.doi.org/10.1021/ja2081907 | *J. Am. Chem.Soc.* 2012, 134, 2094−2099

dried with anhydrous $MgSO_4$, filtered, and concentrated under aspirator pressure. Recyrstallization of the resulting solid from absolute ethanol afforded 11.92 g (79%) of the tribenzyl alcohol as a white solid. ^{1}H NMR (300 MHz, $CDCl_3$) δ 1.51 (1H, s), 2.79 (6H, s), 7.28 (15H, m). ^{13}C NMR (75 MHz, $CDCl_3$) δ 45.7, 73.9, 126.4, 128.1, 131.0, 137.3. HRMS-ESI: calc for $C_{22}H_{22}NaO^+$ $(M + Na)^+$ 325.1563, found 325.1581.

1,3-Di(cyclohexa-1,4-dienyl)-2-(cyclohexa-1,4-dienylmethyl)-propan-2-ol. Tribenzylmethanol (2.00 g, 6.61 mmol) was placed in a 500 mL flask that was equipped with a Claisen adapter and a dry ice−acetone condenser. The reaction flask was charged with 200 mL of liquid ammonia followed by 40 g (0.54 mol) of *tert*-butanol, and then 0.80 g (0.11 mol) of small pieces of lithium wire (Sigma Aldrich) were added over 4 h with stirring. By allowing the reaction mixture to warm to room temperature overnight, the ammonia was evaporated to afford a white solid. It was dissolved in 100 mL of water and extracted three times with 100 mL of diethyl ether. The combined organic layers were dried over $MgSO_4$ and concentrated under reduced pressure, and the crude product was purified by flash column chromatography (20:1 hexanes/diethyl ether) to give 1.54 g (76%) of the desired alcohol as a colorless oil. ^{1}H NMR (300 MHz, $CDCl_3$) δ 1.76 (1H, s), 2.14 (6H, br s), 2.75 (12H, br s), 5.49 (3H, br s), 5.69 (6H, br s). ^{13}C NMR (75 MHz, $CDCl_3$) δ 26.7, 31.1, 48.0, 74.2, 123.1, 123.4, 124.5, 132.2. HRMS-ESI: calc for $C_{22}H_{28}NaO^+$ $(M + Na)^+$ 331.2032, found 331.2029.

5-(2,4-Dihydroxybutyl)nonane-1,3,5,7,9-pentaol (4). A solution of 1.23 g (4.00 mmol) of 1,3-di(cyclohexa-1,4-dienyl)-2-(cyclohexa-1,4-dienylmethyl)propan-2-ol in 100 mL of a 1:1 mixture of methanol/dichloromethane was cooled to −78 °C, and then ozone was bubbled through it for 1 h until a blue color persisted. Excess ozone was removed from the reaction mixture by passing oxygen through it, and then 7.40 g (195 mmol) of sodium borohydride was slowly added with stirring over the course of 1 h, all the while maintaining the temperature at −78 °C. The resulting solution was allowed to warm to room temperature and was maintained at 20 °C for 14 h. Acidification of the reaction mixture was carried out by slowly adding concentrated HCl until the pH was lowered to ∼4 and a white precipitate formed. The resulting methanolic solution was filtered and concentrated at aspirator pressure with a rotary evaporator to afford a residue which was filtered, redissolved in 100 mL of methanol and concentrated again. This step was repeated several times to facilitate the removal of boron-containing compounds as volatile byproducts. The remaining material was purified on a silica gel column by flash chromatography (4:1 ethyl acetate/methanol) to afford 0.29 g (25%) of 5-(2,4-dihydroxybutyl)-nonane-1,3,5,7,9-pentaol as an ∼3: 1 mixture of the anti (RRS/SSR) and syn (RRR/SSS) isomers. ^{1}H NMR (300 MHz, CD_3OD) δ 1.80 (12H, m), 3.68 (6H, t, J = 6.0 Hz), 4.10 (3H, m). ^{13}C NMR (75 MHz, CD_3OD) δ 42.5 (anti), 42.6 (anti and syn), 42.7 (anti), 46.3 (anti), 46.6 (syn), 47.2 (anti), 47.9 (anti), 60.2 (syn), 60.3 (anti), 60.4 (anti), 60.5 (anti), 67.3 (syn), 67.57 (anti), 67.60 (anti), 77.0 (anti), 77.4 (syn); the syn isomer was isolated from its diastereomer by flash chromatography using a 4:1 dichloromethane/methanol solvent mixture after the PES experiments were carried out. HRMS-ESI: calc for $C_{13}H_{28}NaO_7^+$ $(M + Na)^+$ 319.1727, found 319.1732.

Photoelectron Spectroscopy. Photoelectron spectra were obtained at 20 K with a home-built variable temperature photoelectron spectrometer coupled with an electrospray ion source and a cryogenic ion-trap which has been previously described.[6] In this work, the alcohols were dissolved in a methanol/water solution (7:3 v/v) and electrospray ionization of $\sim 10^{-3}$ M solutions afforded the $(M - 1)^-$ ions, except for 1,3-propanediol. The ions were trapped and cooled for a period of 20−80 ms in the trap before being pulsed out into the extraction zone of a time-of-flight mass spectrometer with a repetition rate of 10 Hz. The desired $(M - 1)^-$ ions were mass-selected and decelerated before being intercepted by a probe laser beam in the photodetachment zone of a magnetic bottle photoelectron analyzer. An excimer laser (193 nm, 6.424 eV) and a Nd:YAG laser (266 nm, 4.661 eV) were used in this study, and all three ions were examined at both wavelengths. The laser was operated at a 20 Hz repetition rate with the ion beam off on alternating laser shots to enable shot-by-shot background subtraction to be carried out. Photoelectrons were collected at nearly 100% efficiency with the magnetic bottle and analyzed in a 5.2 m long electron flight tube. Time-of-flight photoelectron spectra were collected and converted to kinetic energy spectra, calibrated by the known spectra of I^- and ClO_2^-. The electron binding energy spectra were obtained by subtracting the kinetic energy spectra from the detachment photon energies. The resolution ($\Delta E/E$) of the resulting spectra was approximately 2% or 20 meV at 1 eV, as measured for I^- at 355 nm. Photoelectron spectra for deprotonated triol **2** and tetraol **3** with the higher energy light source are given in Figure S1 in the Supporting Information.

Computational Methods. Extensive geometry optimizations were previously carried out on all of the anions studied in this work using the Becke three-parameter hybrid exchange and Lee−Yang−Parr correlation density functional (B3LYP)[7] along with the Dunning augmented correlation-consistent double-ζ basis set (aug-cc-pVDZ).[8] In this investigation, the lowest energy structure for each ion was reoptimized using the newer Minnesota 2006 density functional (M06-2X)[9] and served as the starting point for optimizing the structure of the corresponding radical with both functionals. The aug-cc-pVDZ basis set was used as before, but additional M06-2X single-point energies with the maug-cc-pVT(+d)Z basis set (i.e., M06-2X/maug-cc-pVT(+d)Z//M06-2X/aug-cc-pVDZ) were also computed.[10] Vibrational frequencies were calculated in both cases, and the unscaled values provided zero-point energies and thermal corrections to the enthalpies. Vertical detachment energies (VDEs) were calculated by taking the electronic energy differences between the different anions and their corresponding radicals with the same geometries as the ions. Adiabatic detachment energies (ADEs) are reported as enthalpies at 0 K and were obtained using the optimized structures for both the anions and the radicals. All of the other energies reported in this work are given as enthalpies at 298 K. Gaussian 09[11] was used to carry out all of the calculations reported in this study, and the resulting geometries and energies are provided in the Supporting Information.

RESULTS AND DISCUSSION

For an enzyme to catalyze a reaction, it must increase the rate relative to the uncatalyzed background process by reducing the energy difference between the reactant and the transition state. This can be accomplished by destabilizing the energy of the substrate in the enzyme bound complex or by lowering the transition state energy. In a similar manner, the electron binding energy of an anion can be increased by one or more hydrogen bonds if the stabilizing interaction(s) is greater in the ion than in the corresponding radical. To directly probe the effects of hydrogen bonds on a single-charged center, $HOCH_2CH_2CH_2OH$ (**1**), $(HOCH_2CH_2)_2CHOH$ (**2**), and $(HOCH_2CH_2)_3COH$ (**3**) were electrosprayed into a home-built variable temperature photoelectron spectrometer which has been described previously.[6] The $(M - 1)^-$ ions of **2** and **3** (**2a** and **3a**) were produced, but no signal was observed for the diol because it is not much more acidic than methanol.[12] In the triol and tetraol, there are two hydroxyl groups that could be ionized, but deprotonation of the internal one (i.e., the secondary and tertiary alcohol sites in **2** and **3**, respectively) leads to a more favorable hydrogen bonding network (Figure 2). For example, the primary alkoxide derived from the tetraol can only form two hydrogen bonds to the charged site whereas the tertiary alkoxide can form three. This leads to a computed 6.0 kcal mol^{-1} energy difference (B3LYP/aug-cc-pVDZ) between the two isomers, and since they should be able to readily interconvert, it is reasonable to conclude that the ion composition is largely, if not entirely, made up of the more stable anion.

Photoelectron spectra were recorded for **2a** and **3a** at 193 nm (6.424 eV) and 266 nm (4.661 eV) at 20 K, and the latter data are given in Figure 3; the 193 nm spectra have an

dx.doi.org/10.1021/ja2081907 | J. Am. Chem.Soc. 2012, 134, 2094−2099

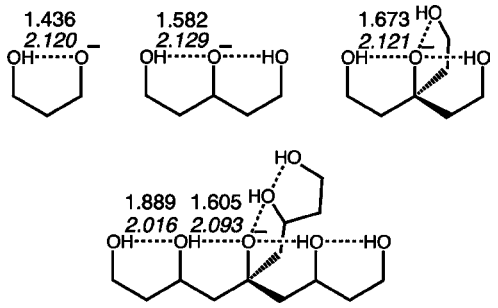

Figure 2. Most favorable hydrogen bonding patterns found for $HOCH_2CH_2O^-$ (**1a**), $(HOCH_2CH_2)_2CHO^-$ (**2a**), $(HOCH_2CH_2)_3CO^-$ (**3a**), and $(HOCH_2CH_2CH(OH)CH_2)_3CO^-$ (**4a**). Bond lengths for the anion and radical (in italics) are in angstroms and are from the M06-2X/aug-cc-pVDZ geometries; the values for **3r**, **4a**, and **4r** are averages of the three different bond distances.

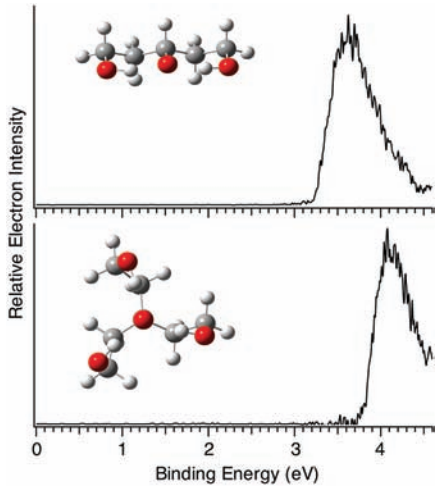

Figure 3. Low temperature (20 K) photoelectron spectra of $(HOCH_2CH_2)_2CHO^-$ (**2a**, top) and $(HOCH_2CH_2)_3CO^-$ (**3a**, bottom) at 266 nm (4.661 eV).

additional band at higher energy corresponding to the formation of the radical in an excited state and are provided in the Supporting Information. The top of the bands in the 266 nm spectra provide the vertical detachment energies (VDEs) of the anions, and a linear extrapolation of the fast rising onset region leads to what should be a good estimate of the adiabatic detachment energies (ADEs).[13] The results are presented in Table 1 along with the literature value for 1-propoxide ($CH_3CH_2CH_2O^-$)[14] and B3LYP predictions with the aug-cc-pVDZ basis set (i.e., B3LYP/aug-cc-pVDZ).[7,8] The newer and apparently superior Minnesota 06 functional of Truhlar et al. was also used,[9] and since the energetics obtained using this method are more sensitive to the basis set, single-point energies were computed using the recently reported minimally augmented triple-ζ+d basis set (i.e., maug-cc-pVT(+d)Z)[10] on the aug-cc-pVDZ geometries (i.e., M06-2X/maug-cc-pVT(+d)Z//M06-2X/aug-cc-pVDZ). In general, both computational methods do well in reproducing the experimental data, but the M06-2X approach with the maug-cc-pVT(+d)Z basis set gives the best results. These values, however, are consistently too small by 0.16 eV (i.e., the errors span from 0.12 to 0.19 eV). As a result, this leads to an estimate of 2.63 eV for the ADE of $HOCH_2CH_2CH_2O^-$.[15]

The differences between the ADEs of the conjugate bases of 1-propanol and the polyols provide a direct measure of the consequences of multiple hydrogen bonds to a single charged center. This is not to say that these energy differences are the hydrogen bond strengths, since there is no way to uniquely partition the various contributions that lead to the overall stability of the ion. In any case, total stabilizations as given by ADE $((HOCH_2CH_2)_nCH_{3-n}O^- - CH_3CH_2CH_2O^-)$ for n = 1−3 lead to 19.4, 34.8, and 47.5 kcal mol^{-1}, respectively, and stabilization energies of 19.4, 17.4, and 15.8 kcal mol^{-1} per hydrogen bond; the latter numbers were obtained from the total stabilizations by dividing them by n, the number of hydrogen bonds in the ion. These findings are in accord with earlier results by Herschlag et al. on ortho-substituted benzoic acids obtained by measuring their pK_a's in dimethysulfoxide (DMSO),[3] our earlier work on the acidities of **1**−**3** in DMSO and the gas phase,[4] and a variety of reports describing the stabilization of polyfunctional ions via hydrogen bonds.[16] Our data herein on simple covalently bound model systems for oxyanion holes with up to three hydrogen bonds reveal that up to 47.5 kcal mol^{-1} is available for catalysis, to the extent that Nature can mimic the gas phase results. The energy gain is 44% of this value, however, if DMSO is used as the reference medium.[17]

To this point, only hydrogen bonds to a charged center are present, but additional interactions between noncharged groups may also contribute to an enzyme's catalytic ability. This can be energetically significant, particularly since hydrogen bond donors to a charged group also will be better hydrogen bond acceptors than they would be in the absence of the charge. A more effective hydrogen bond array, consequently, could result. To assess the energetics that can be brought to bear in such a network, the conjugate base of an alcohol with seven OH groups (i.e., $(HOCH_2CH_2CH(OH)CH_2)_3COH$, **4**) was examined. This ion (**4a**) can be stabilized by a total of six hydrogen bonds, and the most favorable structure that was

Table 1. Experimental and Computed Adiabatic (ADE) and Vertical (VDE) Electron Binding Energies for a Series of Alkoxides in eV

	exptl		calcd[a]	
cmpd (RO^-)	ADE	VDE	ADE	VDE
$CH_3CH_2CH_2O^-$	1.789 ± 0.033		1.66 (1.57) [1.63]	1.81
$HOCH_2CH_2CH_2O^-$ (**1a**)			2.41 (2.40) [2.47]	2.69 (2.87)
$(HOCH_2CH_2)_2CHO^-$ (**2a**)	3.30	3.63	3.07 (3.09) [3.18]	3.53 (3.70)
$(HOCH_2CH_2)_3CO^-$ (**3a**)	3.85	4.18	3.53 (3.58) [3.66]	4.00 (4.18)
$(HOCH_2CH_2CH(OH)CH_2)_3CO^-$ (**4a**)	4.60	5.06	4.28 (4.36) [4.45]	4.76 (5.05)

[a]Computed values are at 0 K and correspond to B3LYP/aug-cc-pVDZ, M06-2X/aug-cc-pVDZ (in parentheses), and M06-2X/maug-cc-pVT(+d)Z//M06-2X/aug-cc-pVDZ (in brackets) energies; the difference between computed values at 0 and 20 K is negligible (i.e., <0.01 eV).

dx.doi.org/10.1021/ja2081907 | J. Am. Chem.Soc. 2012, 134, 2094−2099

computationally located has three hydrogen bonds to the charged center and three additional ones between noncharged OH groups (Figure 2). In this species the internal secondary hydroxyl groups serve as both hydrogen bond donors and acceptors. Conformers with four OH groups interacting with the oxyanion center were located, but the most favorable one is 7.0 (M06-2X/maug-cc-pVT(+d)Z//M06-2X/aug-cc-pVDZ) kcal mol^{-1} less stable than the structure shown in Figure 2 (and Figure 4). This is consistent with a hydration shell number of 3 for hydroxide, as determined by Meot-Ner and Speller.[18]

Heptaol **4** is an unknown compound, but it can be prepared as a mixture of two diastereomers as outlined in Scheme 1. The

Scheme 1. Synthetic Route for the Preparation of Heptaol 4

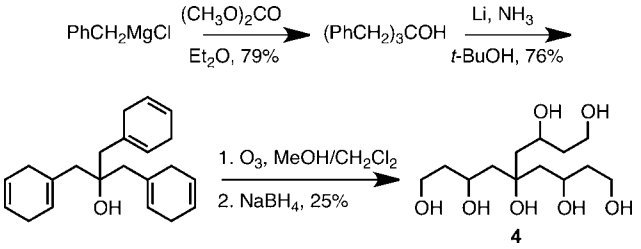

resulting product affords an abundant $(M - 1)^-$ ion signal via electrospray ionization, but irradiation at 266 nm does not lead to electron detachment. A low temperature spectrum at 20 K was recorded (Figure 4), however, when more energetic

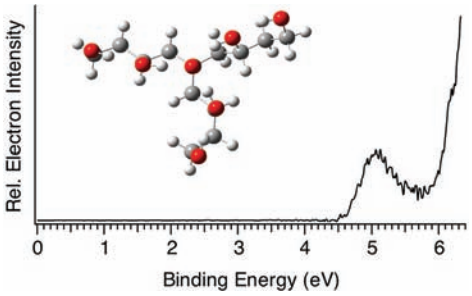

Figure 4. Low temperature (20 K) photoelectron spectrum of $(HOCH_2CH_2CH(OH)CH_2)_3CO^-$ (**4a**) at 193 nm (6.424 eV).

193 nm photons were used. As with the smaller polyol anions at this wavelength, two features are apparent in the spectrum, and the lower energy band provides the adiabatic and vertical electron detachment energies. These values are 4.60 (ADE) and 5.06 eV (VDE), which are remarkably large for a saturated alkoxide anion that lacks electron withdrawing groups and is not stabilized by resonance. To put these record breaking electron detachment energies in context, it is worth noting that the conjugate bases of strong acids such as CH_3CO_2H, HCl, HNO_3, and $HClO_3$ all have smaller ADEs (i.e., 3.470 ± 0.010, 3.613577 ± 0.000044, 3.937 ± 0.014, and 4.25 ± 0.10 eV, respectively)[19−22] than the deprotonated heptaol, whereas dihydrogen phosphate ($H_2PO_4^-$) has essentially the same value (i.e., 4.570 ± 0.010 eV).[23]

The hydrogen bond array in the conjugate base of **4** leads to a 64.8 kcal mol^{-1} stabilization relative to $CH_3CH_2CH_2O^-$, and 17.3 kcal mol^{-1} compared to the $(M - 1)^-$ ion of tetraol **3**. The latter difference can be attributed to the additional contribution from the three enhanced hydrogen bonds between the noncharged OH groups. These intramolecular interactions and those in the conjugate bases of **1**−**3** can be compared to the intermolecular hydrogen-bonded networks in $OH^-(H_2O)_n$, where n = 1−6 (Figure 5 and Table 2).[18,24,25] As can be seen

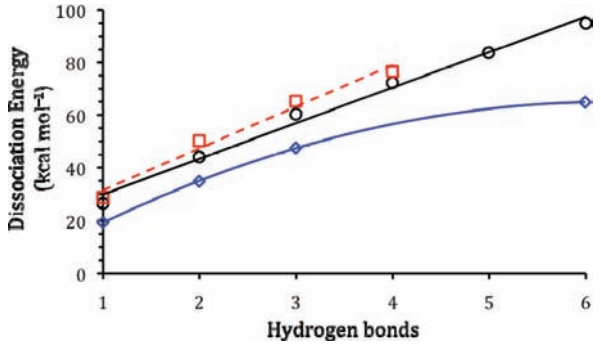

Figure 5. Dissociation energies versus hydrogen bond numbers. Diamonds are for polyol $(M - 1)^-$ ion ΔADEs relative to CH_3CH_2-CH_2O^- (blue), circles represent the total dehydration energies of $OH^-(H_2O)_n$ (black), and squares are for the $CH_3O^-(CH_3OH)_n$ cluster energies (red).

Table 2. Energetic Consequences of Intramolecular vs Intermolecular Hydrogen Bonds[a]

n	ΔADE/n (intramolecular)	$\Delta H°(RO^-(ROH)_n \rightarrow RO^- + nROH)/n$, R = H and CH_3 (intermolecular)[b]	intramol/intermol (%)[c]
1	(**1a** − $CH_3(CH_2)_2O^-$)/n = 19.4	26.5 [28.8]	73
2	(**2a** − **1a**)/n = 17.4	22.1 [25.1]	79
3	(**3a** − **1a**)/n = 15.8	20.1 [21.7]	79
4		12.0 [11.4]	
5		11.8	
6	(**4a** − **3a**)/(n − 3) = 5.8	11.6	50

[a]All of the energies are in kcal mol^{-1}. [b]These data come from refs 18 and 24, and the first value is for R = H and the latter one (in brackets) is for R = CH_3. When $n \geq 4$, then the given energies are for $\Delta H°(RO^-(ROH)_n \rightarrow RO^-(ROH)_3 + mROH)/m$, where $m = n - 3$. [c]The water cluster intermolecular values were used for this comparison.

for n = 1−3 in Figure 5, the intramolecular hydrogen bond system mirrors the intermolecular interaction energies closely but is ∼20−25% smaller. This is presumably because of geometric constraints in the polyols that restrict the O−H···O hydrogen bond angles from the ideal value of 180° to 153.0−158.5° (B3LYP) or 151.0−160.4° (M06-2X) when n = 1−3. The energy gap in Figure 5 is larger for n = 6, and it is tempting to attribute this to water−water interactions in $OH^-(H_2O)_6$, especially since computations indicate that the water molecules hydrogen bond with each other when $n \geq 3$.[26] Methoxide−methanol cluster energies (the squares in Figure 5),[24] however, follow the same trend as the hydroxide−water complexes even though the hydrogen-bonded network is more limited in the former case, since alcohols have one less O−H bond than in water. This suggests that the fall off for **4a** is not due to water−water interactions in $OH^-(H_2O)_6$ but is instead the result of its more limited conformational flexibility. In accord with this hypothesis, the computed O−H···O hydrogen bond angles between the terminal hydroxyl groups and the oxygen atoms of the internal hydroxyl groups are 144−145° (B3LYP) and 142−143° (M06-2X) or ∼10−15° smaller than the O−H···O$^-$ angles in **1a**−**4a**. This leads to weaker hydrogen bonds in the outer

dx.doi.org/10.1021/ja2081907 | J. Am. Chem.Soc. 2012, 134, 2094−2099

shell of **4a** that presumably can be strengthened by increasing the flexibility in **4** (e.g., by adding a CH_2 spacer between the primary and secondary OH groups).

Enzyme–substrate complexes enjoy a kinetic advantage over bimolecular processes because intramolecular reactions are generally favored over intermolecular ones.[27] Our simple covalently bound models for the former species reveal that hydrogen-bonded networks can be stabilized by the presence of a charged site, and this thermodynamic effect can be used to perturb acidities and basicities and catalyze enzyme reactions.[28] As a result, aqueous pK_a values may be a poor indication of the acidity or basicity of a given group in a biological context, and proton transfer processes that are currently viewed as being energetically unfavorable and inaccessible actually may take place. Careful control of hydrogen-bonded networks consequently is an attractive design strategy for molecular recognition and artificial enzyme construction.[29]

CONCLUSIONS

The photoelectron spectra of a series of deprotonated polyhydroxyalcohols were obtained at 20 K, and the adiabatic electron detachment energies for $HOCH_2CH_2CH_2O^-$ (**1a**), $(HOCH_2CH_2)_2CHO^-$ (**2a**), $(HOCH_2CH_2)_3CO^-$ (**3a**), and $(HOCH_2CH_2CH(OH)CH_2)_3CO^-$ (**4a**) are 2.63 (best estimate, see text for details), 3.30, 3.85, and 4.60 eV, respectively. These values are remarkably large and are bigger than the experimental ADE for $CH_3CH_2CH_2O^-$ (1.789 ± 0.033 eV) by 19.4, 34.8, 47.5, and 64.8 kcal mol^{-1}. These energy differences are a consequence of the hydrogen-bonded networks in the anions, and in the case of **4a** this leads to an ADE that is greater than those of the conjugate bases of CH_3CO_2H, HCl, and HNO_3. Its ADE is also 17.3 kcal mol^{-1} or 5.8 kcal mol^{-1} per hydrogen bond greater than that for **3a**, and this difference can be attributed to the enhanced strength of the three hydrogen bonds between the noncharged OH groups in **4a**. The presence of a charged center leads to a considerable increase in the strength of a hydrogen-bonded network, and this undoubtedly plays a key role in regulating the structure and function of a wide range of biomolecules.

ASSOCIATED CONTENT

Supporting Information

Computed geometries and energies, along with the 20 K photoelectron spectra of **2a** and **3a** at 193 nm (6.424 eV) and the complete citation to ref 11. This material is available free of charge via the Internet at http://pubs.acs.org.

AUTHOR INFORMATION

Corresponding Author

kass@umn.edu; xuebin.wang@pnnl.gov

ACKNOWLEDGMENTS

This work is dedicated to the memory of Donna Kass. Generous support from the National Science Foundation, the Petroleum Research Fund, and the Minnesota Supercomputer Institute for Advanced Computational Research are gratefully acknowledged. The photoelectron spectra work was supported by the Division of Chemical Sciences, Geosciences and Biosciences, Office of Basic Energy Sciences, U.S. Department of Energy (DOE), and performed at the Environmental Molecular Sciences Laboratory (EMSL), a national scientific user facility sponsored by DOE's Office of Biological and Environmental Research and located at Pacific Northwest National Laboratory, which is operated by Battelle for the DOE. We also thank Prof. Brian Miller for helpful suggestions.

REFERENCES

(1) (a) Childs, W.; Boxer, S. G. *Biochemistry* **2010**, *49*, 2725–2731. (b) Simon, L.; Goodman, J. M. *J. Org. Chem.* **2010**, *75*, 1831–1840. (c) Sigala, P. A.; Kraut, D. A.; Caaveiro, J. M. M.; Pybus, B.; Rubin, E. A.; Ringe, D.; Petsko, G. A.; Herschlag, D. *J. Am. Chem. Soc.* **2008**, *130*, 13696–13708. (d) Zhang, Y.; Kua, J.; McCammon, J. A. *J. Am. Chem. Soc.* **2002**, *124*, 10572–10577. (e) Whiting, A. K.; Peticolas, W. L. *Biochemistry* **1994**, *33*, 552–561.

(2) (a) Gerlt, J. A.; Gassman, P. G. *Biochemistry* **1993**, *32*, 11943–11952. (b) Gerlt, J. A.; Gassman, P. G. *J. Am. Chem. Soc.* **1993**, *115*, 11552–11568. (c) Cleland, W. W.; Kreevoy, M. M. *Science* **1994**, *264*, 1887–1890. (d) Frey, P. A.; Whitt, S. A.; Tobin, J. B. *Science* **1994**, *264*, 1927–1930. (e) Cleland, W. W.; Frey, P. A.; Gerlt, J. A. *J. Biol. Chem.* **1998**, *273*, 25529–25532. (f) Schwans, J. P.; Kraut, D. A.; Herschlag, D. *Proc. Natl. Acad. Sci. U. S. A.* **2009**, *106*, 14271–14275.

(3) (a) Shan, S. O.; Herschlag, D. *Proc. Natl. Acad. Sci. U. S. A.* **1996**, *93*, 14474–14479. (b) Shan, S. O.; Herschlag, D. *J. Am. Chem. Soc.* **1996**, *118*, 5515–5518. (c) Shan, S. O.; Loh, S.; Herschlag, D. *Science* **1996**, *272*, 97–101. (d) Shan, S. O.; Herschlag, D. *Methods Enzymol.* **1999**, *308*, 246–276.

(4) Tian, Z.; Fattahi, A.; Lis, L.; Kass, S. R. *J. Am. Chem. Soc.* **2009**, *131*, 16984–16988.

(5) (a) Jencks, W. P. *Adv. Enzymol. Relat. Areas Mol. Biol.* **1975**, *43*, 219–410. (b) Jencks, W. P. *Methods Enzymol.* **1989**, *171*, 145–164.

(6) Wang, X. B.; Wang, L. S. *Rev. Sci. Instrum.* **2008**, *79*, 073108.

(7) (a) Becke, A. D. *J. Chem. Phys.* **1993**, *98*, 5648–5652. (b) Lee, C.; Yang, W.; Parr, R. G. *Phys. Rev. B* **1988**, *37*, 785–789.

(8) Dunning, T. H. Jr. *J. Chem. Phys.* **1989**, *90*, 1007–1023.

(9) (a) Zhao, Y.; Truhlar, D. G. *J. Phys. Chem. A* **2008**, *112*, 1095–1099. (b) Zhao, Y.; Truhlar, D. G. *Theor. Chem. Acc.* **2008**, *120*, 215–241. (c) Zhao, Y.; Truhlar, D. G. *Acc. Chem. Res.* **2008**, *41*, 157–167.

(10) Papajak, E.; Truhlar, D. G. *J. Chem. Theory Comput.* **2010**, *6*, 597–601.

(11) Frisch, M. J., et al.. *Gaussian 09*; Gaussian, Inc.: Pittsburgh, PA, 2009.

(12) Woolley, E. M.; Tomkins, J.; Hepler, L. G. *J. Solution Chem.* **1972**, *1*, 341–351.

(13) Vibrational resolution is required to obtain a precise value for the electron affinity, but given that the anion and radical geometries are predicted to be in similar bonding configurations, we anticipate that the adiabatic electron affinities reported herein are accurate to within 0.10 eV. Our M06-2X computations on **1a**–**4a** indicate, however, that the OH···O$^-$ distances increase upon formation of their radicals, as one would expect.

(14) Ellison, G. B.; Engleking, P. C.; Lineberger, W. C. *J. Phys. Chem.* **1982**, *86*, 4873–4878.

(15) Both the B3LYP and M06-2X ADEs with the aug-cc-pVDZ basis set are also underestimated, but in these cases, the average error is 0.23 eV. This leads to corrected predictions of 2.64 (B3LYP) and 2.63 eV (M06-2X) for $HOCH_2CH_2CH_2O^-$, which are the same as the M06-2X/maug-cc-pVT(+d)Z value given in the text (to within 0.01 eV).

(16) For examples, see: (a) Tian, Z.; Fattahi, A.; Lis, L.; Kass, S. R. *Croat. Chem. Acta* **2009**, *82*, 41–45. (b) Meot-Ner (Mautner), M. *Chem. Rev.* **2005**, *105*, 213–284.

(17) This percentage is the average of $pK_a(\mathbf{2}-\mathbf{3})_{DMSO}/\Delta G^\circ_{acid}(\mathbf{2}-\mathbf{3})_{gas\ phase}$ and $pK_a(\mathbf{3}-\mathbf{4})_{DMSO}/\Delta G^\circ_{acid}(\mathbf{3}-\mathbf{4})_{gas\ phase}$, where the experimental values come from ref 4.

(18) Meot-Ner (Mautner), M.; Speller, C. V. *J. Phys. Chem.* **1986**, *90*, 6616–6624.

(19) Lu, Z.; Continetti, R. E. *J. Phys. Chem. A* **2004**, *108*, 9962–9969.

(20) Berzinsh, U.; Gustafsson, M.; Hanstorp, D.; Klinkmuller, A.; Ljungblad, U.; Martensson-Pendrill, A. M. *Phys. Rev. A* **1995**, *51*, 231–238.

(21) Weaver, A.; Arnold, D. W.; Bradforth, S. E.; Neumark, D. M. *J. Chem. Phys.* **1991**, *94*, 1740−1751.
(22) Wang, X. B.; Wang, L. S. *J. Chem. Phys.* **2000**, *113*, 10928−10933.
(23) Wang, X. B.; Vorpagel, E. R.; Yang, X.; Wang, L. S. *J. Phys. Chem. A* **2001**, *105*, 10468−10474.
(24) Meot-Ner (Mautner), M. *J. Am. Chem. Soc.* **1986**, *108*, 6189−6197.
(25) For related studies that report multiple intramolecular hydrogen bonding interactions, see: (a) Wu, R.; McMahon, T. B. *J. Phys. Chem. B* **2009**, *113*, 8767−8775. (b) Wu, R.; McMahon, T. B. *J. Am. Chem. Soc.* **2007**, *129*, 11312−11313. (c) Norrman, K.; McMahon, T. B. *J. Phys. Chem. A* **1999**, *103*, 7008−7016. (d) Meot-Ner (Mautner), M.; Sieck, L. W.; Scheiner, S.; Duan, X. *J. Am. Chem. Soc.* **1994**, *116*, 7848−7856. (e) Campbell, S.; Rodgers, M. T.; Marzluff, E. M.; Beauchamp, J. L. *J. Am. Chem. Soc.* **1995**, *117*, 12840−12854. (f) Sharma, R. B.; Blades, A. T.; Kebarle, P. *J. Am. Chem. Soc.* **1984**, *106*, 510−516. (g) Meot-Ner (Mautner), M. *J. Am. Chem. Soc.* **1983**, *105*, 4906−4911.
(26) Xantheas, S. S. *J. Am. Chem. Soc.* **1995**, *117*, 10373−10380.
(27) Bruice, T. C.; Pandit, U. K. *Proc. Natl. Acad. Sci. U.S.A.* **1960**, *46*, 402−404.
(28) Ionic hydrogen bond networks were modeled for the trypsin active site and were found to contribute 65 kcal mol^{-1} in the resting state conformation and 32 kcal mol^{-1} in the transition structure. For more details, see: Meot-Ner (Mautner), M. *J. Am. Chem. Soc.* **1988**, *110*, 3075−3080.
(29) For reviews, see: (a) Joyce, L. A.; Shabbir, S. H.; Anslyn, E. V. *Chem. Soc. Rev.* **2010**, *39*, 3621−3632. (b) Takemoto, Y. *Yuki Gosei Kagaku Kyokaishi* **2006**, *64*, 1139−1147. (c) Schreiner, P. R. *Chem. Soc. Rev.* **2003**, *32*, 289−296. (d) Betschmann, P.; Lerner, C.; Sahli, S.; Obst, U.; Diederich, F. *Chimia* **2000**, *54*, 633−639.